# RECENT NA49 RESULTS ON PB+PB COLLISIONS AT CERN SPS

FERENC SIKLÉR FOR THE NA49 COLLABORATION
*KFKI Research Institute for Particle and Nuclear Physics, Budapest, Hungary*
*E-mail: sikler@rmki.kfki.hu*

In the spirit of establishing a fair reference for nucleus-nucleus collisions, results on stopping and baryon transfer, correlations of the p+p interaction and their consequences are shown. In the discussion of new results from nucleus-nucleus collisions the emphasis is on strange meson and baryon production at different energies – for the first time at 40 GeV·$A$ – with the study of light nuclei.

## 1 Motivation

We study nuclear reactions in order to elucidate the strong interaction process and study its development in time and space with the hope to learn the characteristics of hot and dense matter, moreover to establish experimental links between elementary and complex interactions.

## 2 The experiment

The NA49 experiment is a large acceptance detector for charged hadrons[1]. The tracking of particles is based on four large volume time projection chambers, the particle identification is possible via the measurement of their specific energy loss ($dE/dx$).

One of the key parameters in the systematics of hadron production is the centrality of the collision: the number of collisions per participant nucleon. In case of p+A reactions the centrality is known to be correlated with the number of "grey" particles – slow protons and deuterons – which are measured by a centrality detector surrounding the target and by the tracking system. In Pb+Pb reactions the deposited energy in the zero degree calorimeter was used to select events with given centrality. Both measures were then correlated with the average number of collisions a nucleon undergoes, using simulation.

The data presented here are preliminary results from p+p, p+Al, p+Pb and C+C, Si+Si, Pb+Pb reactions at 158 GeV·$A$ and from Pb+Pb reactions at 40 GeV·$A$ energy.

## 3 Stopping and baryon transfer

The longitudinal momentum distribution of net protons from non-single-diffractive p+p interactions has been measured in the rest frame of the collision (Feynman-x distribution, $x_{_F}$). This can be compared to the measurements of the net proton distribution in centrality selected p+A reactions (Fig. 1.a). With increasing centrality (increasing average number of collisions) the final state protons appear to be more and more stopped with the biggest effect in the most central sample. The evolution is smooth, connecting p+p via p+Al to p+Pb.[a]

In A+A collisions a similar gradual evolution of stopping is seen (Fig. 1.b), although not reaching the high level observed in most central p+Pb.

## 4 Correlations in p+p, predictions

A very characteristic systematics of the net proton distribution as function of $\bar{\nu}$ is observed in p+A and A+A reactions. What about p+p collisions? Although here $\nu = 1$ by definition, the degree of inelasticity of the interaction can be characterized by the $x_{_F}$ of the final state proton. This is exemplified in the following by inspecting the correlations of hadronic variables with $x_{_F}^p$.

### *4.1 Pion density*

The average number of charged pions $\langle\pi\rangle$ strongly correlates with the $x_{_F}$ of the final state proton (Fig. 2.a): a fast proton will be accompanied by a few, a slow one by many pions.

Using the $\langle\pi\rangle$ – $x_{_F}^p$ correlation measured in p+p, predictions can be made for other reactions by folding their – above discussed – proton distribution with this correlation curve. For a reaction that has slower protons one would extrapolate bigger pion density. This is what happens in more and more central Pb+Pb collisions: the observed increase of pion density with centrality is close to the prediction from p+p interactions (Fig. 2.b).

### *4.2 Strangeness content*

As another example, a similar study can be performed with the $\phi(1020)$ meson that carries hidden strangeness. The ratio $\phi/\pi^-$ in the forward hemisphere increases if the event has a slower proton (Fig. 3.a). This leads to a prediction of $\phi$ enhancement in p+A that is in agreement with the data (Fig. 3.b).

[a] Note the similarity of p+Al and p+Pb in the overlap region at $\bar{\nu} \approx 3$.

## 5 A+A strangeness

The 10% most central Pb+Pb collisions have been used. $\Xi^-$ hyperons decay via the channel $\Xi^- \to \Lambda\pi^-$ with the subsequent decay $\Lambda \to p\pi^-$ following. They are found by reconstructing the decay vertices starting with the $\Lambda$ decay vertex. The analyses of $\Lambda(1520)$ and $\phi(1020)$ employ an alternative method of signal extraction. Here, the signal has been extracted from the invariant mass spectra after a procedure of mixed event background subtraction. Corrections for geometrical acceptance, branching ratio and reconstruction efficiency have been applied.

### *5.1* $\Xi^-$ *analysis*

Transverse mass (Fig. 4) and rapidity distributions (Fig. 5) are shown here. Integrating the Gaussian fits over the full rapidity range gives total yields of $4.42 \pm 0.31$ and $0.74 \pm 0.04$ particles per event for $\Xi^-$ and $\overline{\Xi}^+$ respectively. The $\Xi^-/\overline{\Xi}^+$ ratio at midrapidity is found to be $0.22 \pm 0.04$ in good agreement with our previous publication and other experiment[2]. The integrated ratio is $0.17 \pm 0.02$.

### *5.2* $\Lambda(1520)$ *analysis*

Preliminary invariant mass distribution for the $\Lambda(1520) \to p + K^-$ channel for p+p and Pb+Pb collisions is obtained. In the case of p+p collisions the corrected yield amounts to $0.0012 \pm 0.003$ per event. Scaling the p+p yield by the number of participants to central Pb+Pb collisions, the expectation would be $0.012 \times (350/2) \approx 2.1\Lambda(1520)$ per event. At the same time in Pb+Pb only a weak signal is seen which may hint a possible suppression.

### *5.3* $\phi(1020)$ *analysis*

Invariant mass distributions for the $\phi(1020) \to K^+ + K^-$ channel in Pb+Pb and p+p collisions are obtained. No shift in the position or significant broadening of the mass peak is observed. Inverse slopes of $305 \pm 15$ and $169 \pm 17$ MeV, integrated yields of $7.6 \pm 1.1$ and $0.012 \pm 0.0015$ per event are found for central Pb+Pb and inelastic p+p reactions respectively. This indicates a factor of 3 enhancement[3].

## 6 Energy dependence

In order to explore the energy range between top AGS and top SPS energies an energy scan has been started. The importance of this study is supported by a statistical approach that predicts the appearance of a phase transition to quark-gluon plasma in the early stage of nucleus-nucleus collisions in this energy range. In the following the results of the preliminary analysis of 100k reconstructed central Pb+Pb events at 40 GeV·$A$ beam energy are presented.

The excitation function of $K^+$ show peak around 40 GeV·$A$ (Fig. 7). The increase of $K^-/\pi^-$ is continuous. The energy dependence of the ratio of mean pion multiplicity to the number of participating nucleons (Fig. 8.a) and the dependence of strangeness production (Fig. 8.b) are shown with the prediction of the statistical model of the early state[4].

It is observed that the pion yield per participant ratio follows the established trend of low energy data. The strangeness content of the event ($E_S$) in Pb+Pb collisions at 40 GeV·$A$ is higher by about 30% than the corresponding ratios at top AGS and SPS energies. This results may be the first indication of a non-monotonic energy dependence of the strangeness to pion ratio.

RQMD shows similar tendency of central yields[b] but fails for total ones[5].

## 7 System size dependence

Both AGS and SPS experiments observe particle ratios that show smooth dependence on the centrality of the nucleus-nucleus collision, that is, on the number of participants ($N_{part}$). On the other hand, for comparison of interactions of nuclei of different size, $N_{part}$ does not seem to be the right variable, particle ratios do not scale with the volume of the reaction zone (Fig. 9, new points for C+C and Si+Si are from our preliminary analysis).

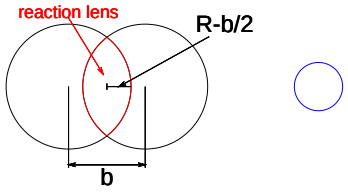


Figure 10. Some geometry, the nuclei move inward and outward.

Here a new scaling measure, the thickness of the reaction zone is proposed. Using the cross section and perimeter of the reaction lens, the volume to surface ratio can be well approximated to be $V/A \approx \frac{2}{3}(R - b/2)$ which can be regarded as the average escape pathlength from the reaction volume (Fig. 10[c]). The impact

[b] The authors state that the strangeness increase is mainly due to rescattering of mesons with baryons. Compare this to the thickness-scaling found in section 7.

[c] The central collision of small nuclei (right) produces as much kaons as the large one at medium impact (left).

parameter $b$ can be estimated via the energy deposited in the zero degree calorimeter. Plotting the above measures against $R - b/2$ all the four central values (C+C, Si+Si, S+S, Pb+Pb) and even the Pb+Pb centrality selected points are closely on the same curve, a line (Fig. 11). There are indications that the increase of transverse momentum for protons is already present for C+C and Si+Si collisions.

## 8 Summary

The NA49 experiment identifies particles in the forward hemisphere with controlled centrality. Hadronic reactions with different targets, projectiles and energies are studied.

Using the internal structure of the p+p interaction, predictions can be made for p+A and A+A collisions. This is to be confronted with the usual method of comparing with minimum bias p+p collision.

New results from Pb+Pb collisions explore the characteristics of $\Xi^-$, $\overline{\Xi}^+$, $\Lambda(1520)$ and $\phi(1020)$ production. Our energy scan opens up the exciting range of lower energy collisions (40 GeV $\cdot A$) which has the highest strangeness content observed so far. New studies with light nuclei help to fill the desert between elementary p+p interactions and Pb+Pb collisions. Already semi-central C+C collisions shows increase of strangeness. An interesting scaling with the thickness of the reaction zone is revealed.

## References


1. S.V. Afanasiev *et al.*, [NA49], *Nucl. Instrum. Methods* A **430**, 210 (1999).
2. R.A. Barton for the NA49 Collaboration, *Proc. of Strangeness 2000.*
3. S.V. Afanasiev *et al.*, [NA49], *Phys. Lett.* B **491**, 59 (2000).
4. M. Gaździcki, M. I. Gorenstein, *Acta Phys. Pol.* B **30**, 2705 (1999).
5. F. Wang, H. Liu, H. Sorge, N. Xu and J. Yang, *nucl-th/9909001.*

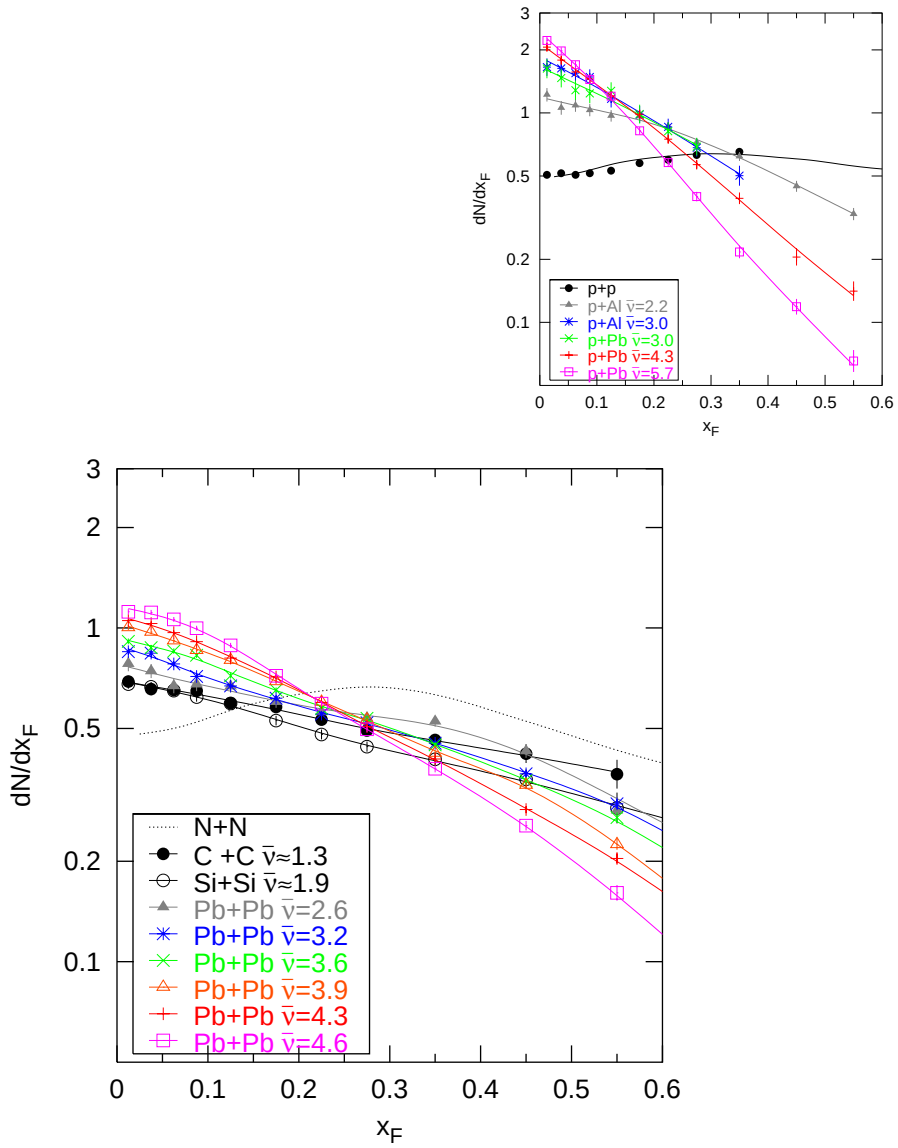


Figure 1. Feynman-x distribution of net protons ($p - \bar{p}$) with different average number of collisions ($\bar{\nu}$) in *a)* p+A and *b)* A+A collisions. Lines are to guide the eye.

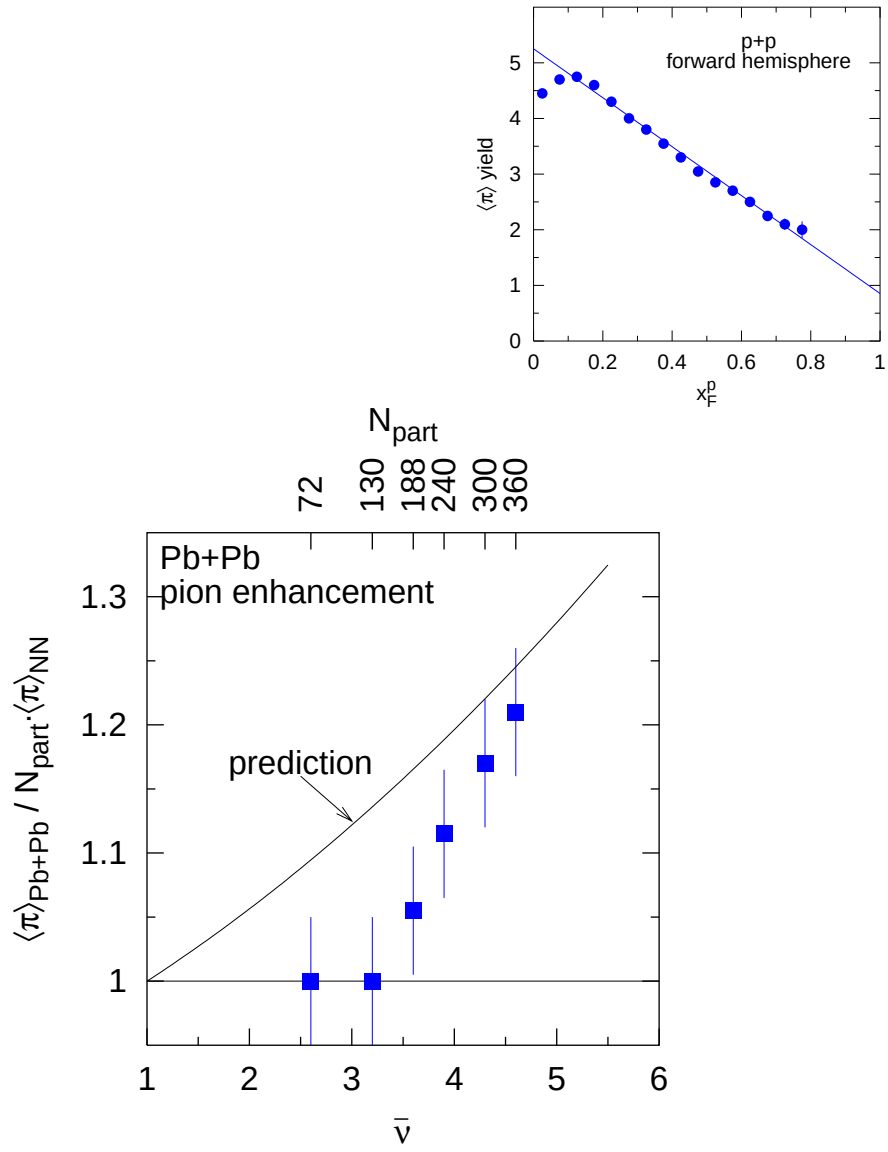


Figure 2. *a)* Average number of charged pions ($\langle\pi\rangle = (\pi^+ + \pi^-)/2$) in the forward hemisphere in p+p collision if the fastest proton has longitudinal momentum $x_F^p$. *b)* Pion enhancement in Pb+Pb collisions relative to minimum bias p+p as function of $\bar{\nu}$. Measured points and predicted line using p+p correlations are shown

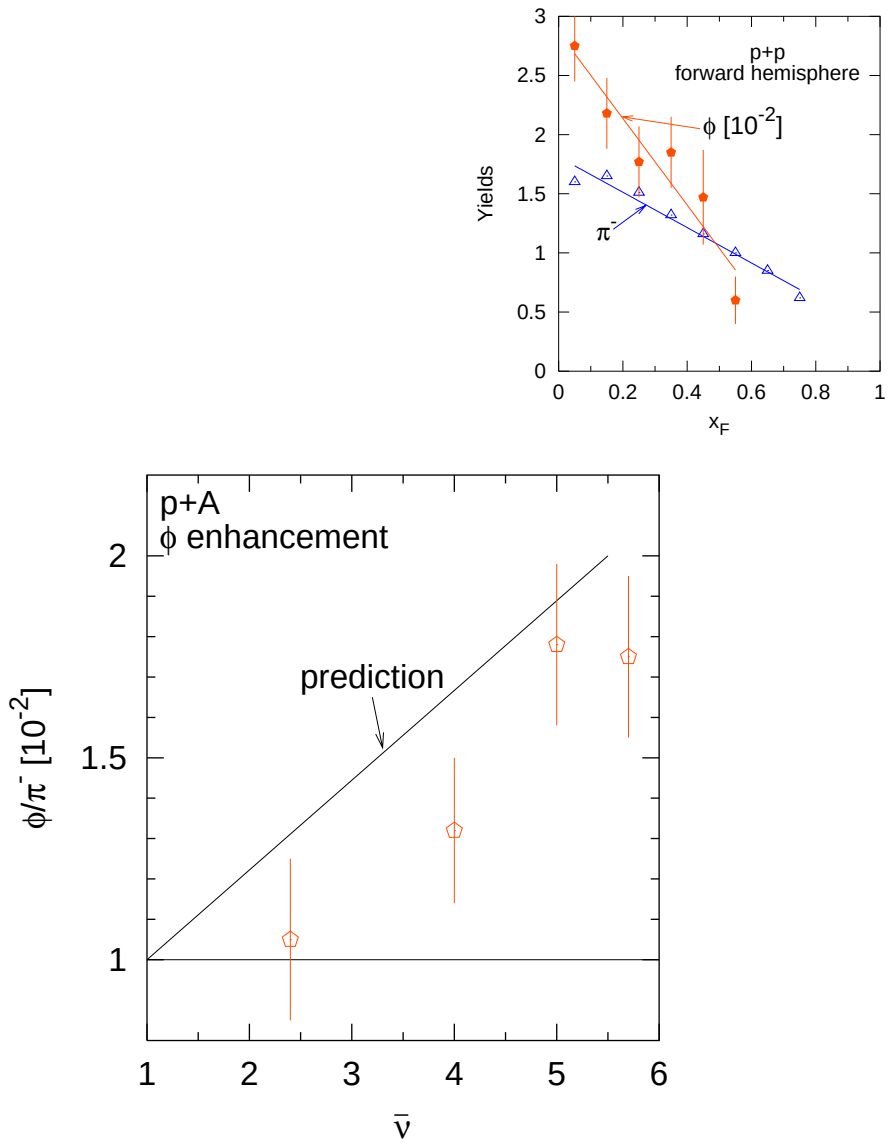


Figure 3. *a)* Yields of negative pions and $\phi$ in the forward hemisphere in p+p collision if the fastest proton has longitudinal momentum $x_F^p$. *b)* $\phi$ enhancement in p+A collisions in the forward hemisphere as function of $\bar{\nu}$. Measured points and predicted line using p+p correlations are shown. The enhancement for central Pb+Pb is at 3.

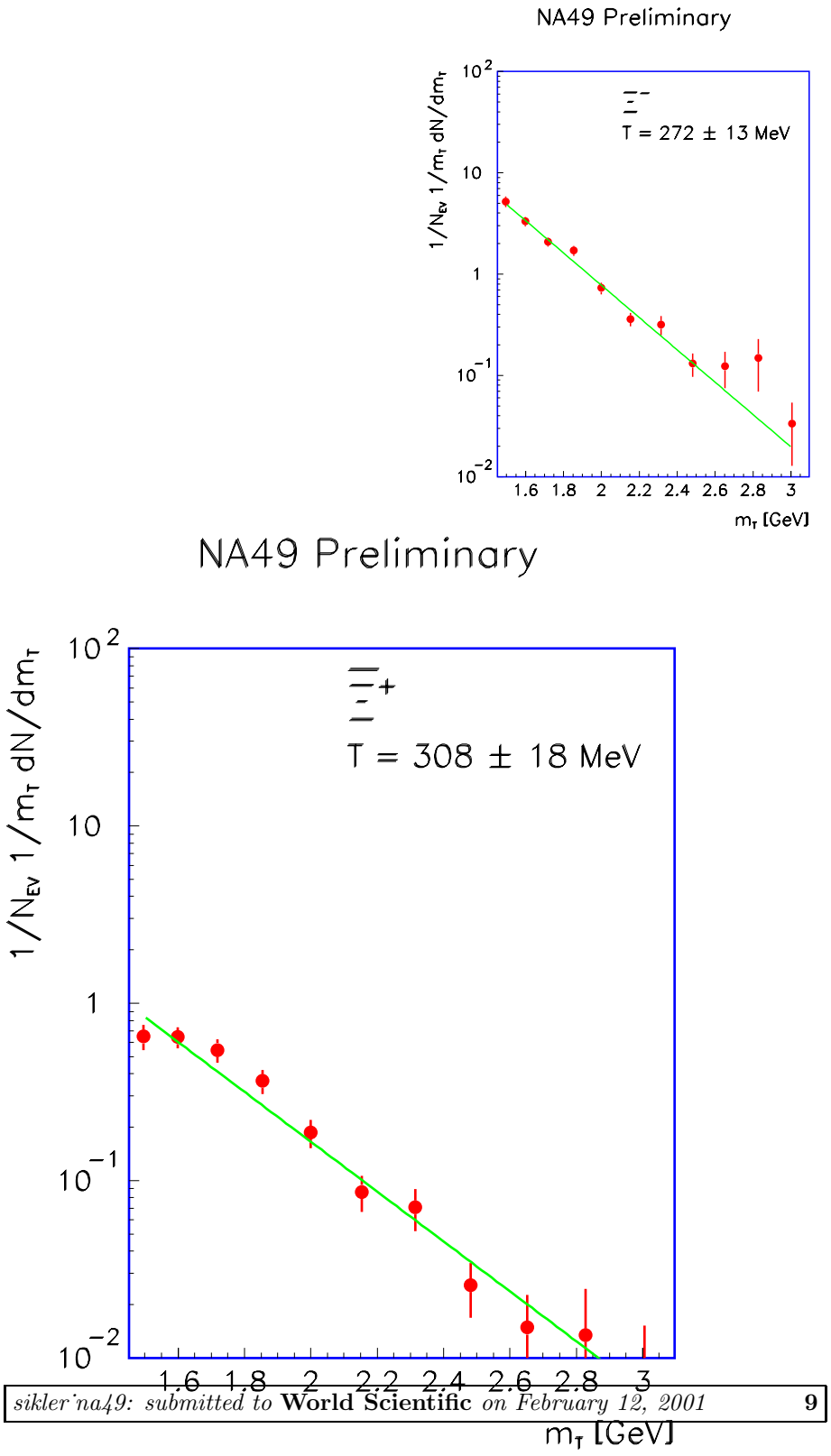




Figure 4. Transverse mass distributions for $\Xi^-$ (left) and $\overline{\Xi}^+$ (right) from central Pb+Pb collisions. Inverse slope parameters are also given.

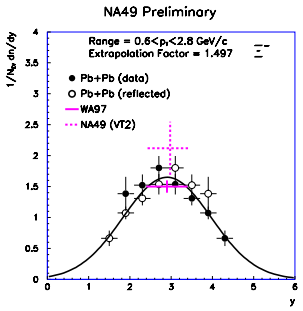
NA49 Preliminary
Range = 0.6<p_T<2.8 GeV/c
Extrapolation Factor = 1.497
Pb+Pb (data)
Pb+Pb (reflected)
WA97
NA49 (VT2)
1/N_ev dn/dy
y

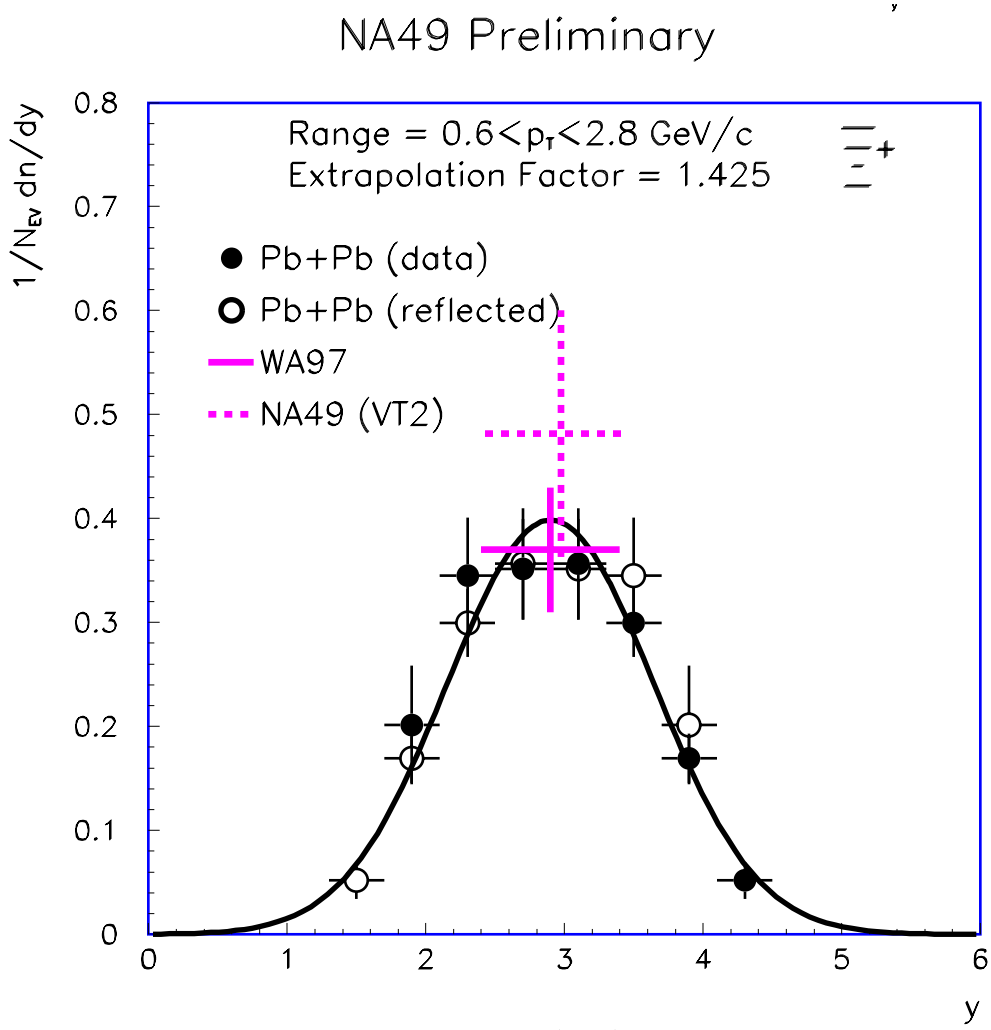
NA49 Preliminary
Range = 0.6<p_T<2.8 GeV/c
Extrapolation Factor = 1.425
Pb+Pb (data)
Pb+Pb (reflected)
WA97
NA49 (VT2)
1/N_ev dn/dy
y

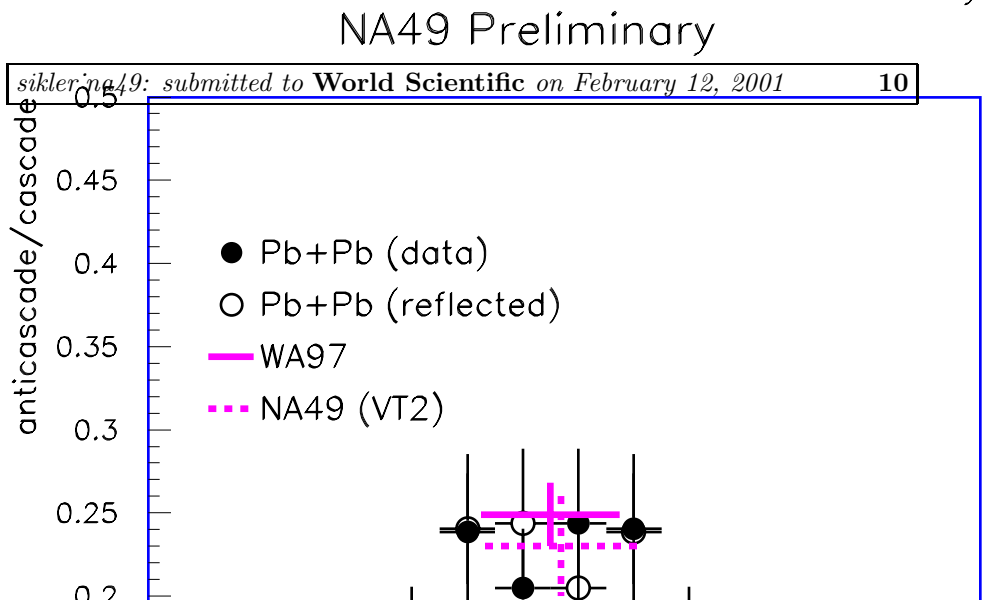
NA49 Preliminary
Pb+Pb (data)
Pb+Pb (reflected)
WA97
NA49 (VT2)
anticascade/cascade

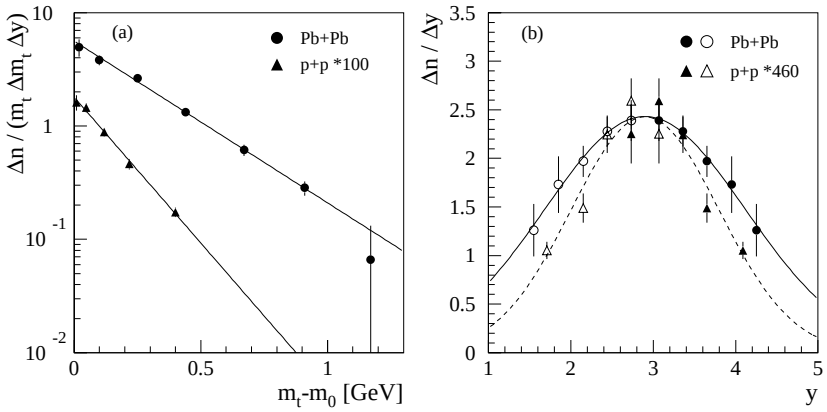


Figure 6. $\phi$ mesons in central Pb+Pb and minimum bias p+p collisions: *a)* transverse mass distributions around midrapidity; *b)* rapidity distributions (full symbols represent measured points, open ones are reflected about midrapidity).

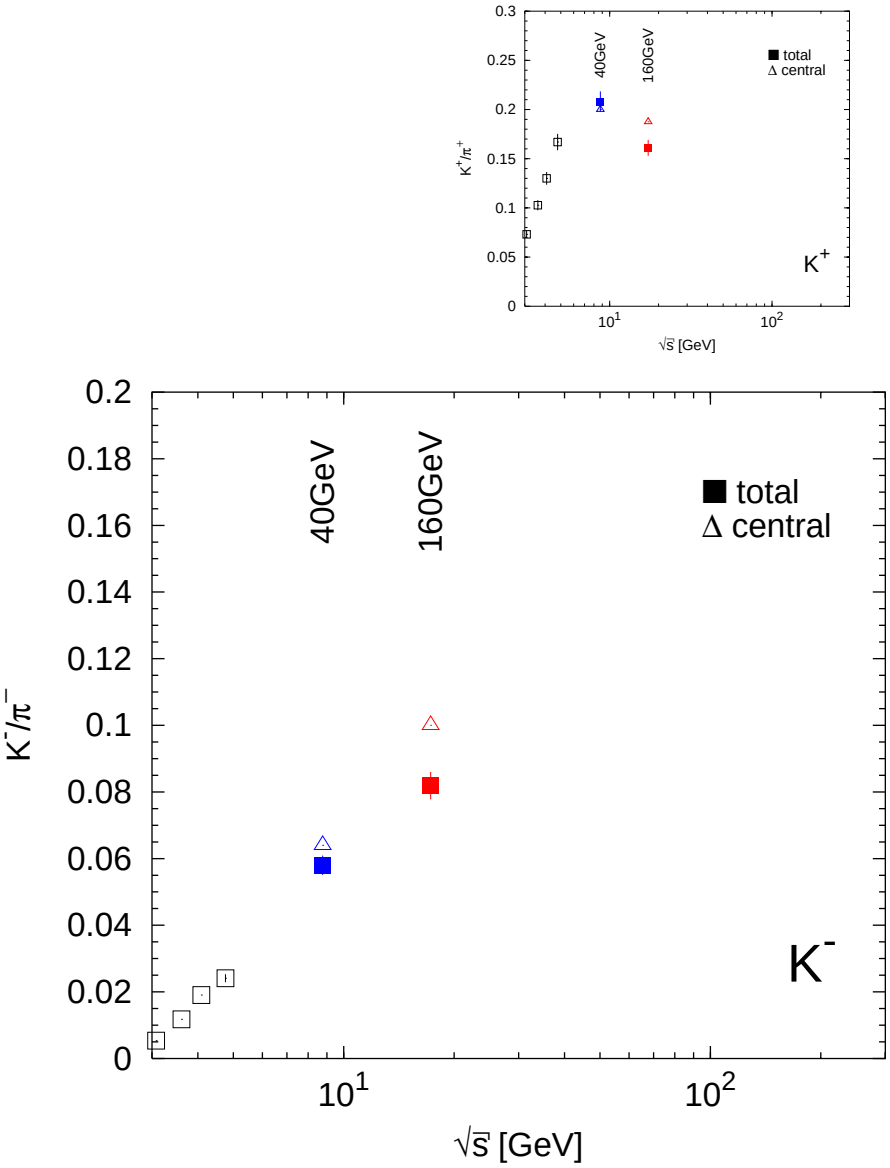


Figure 7. Ratios of $K^+/\pi^+$ and $K^-/\pi^-$ yields as function of collision energy. Closed boxes represent total yields, closed triangles are for central yields.

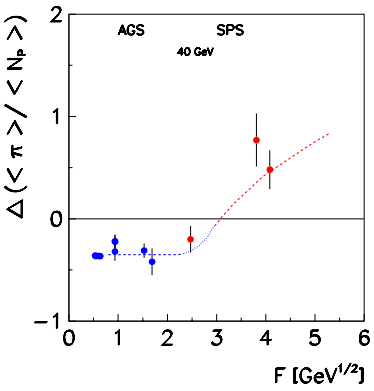


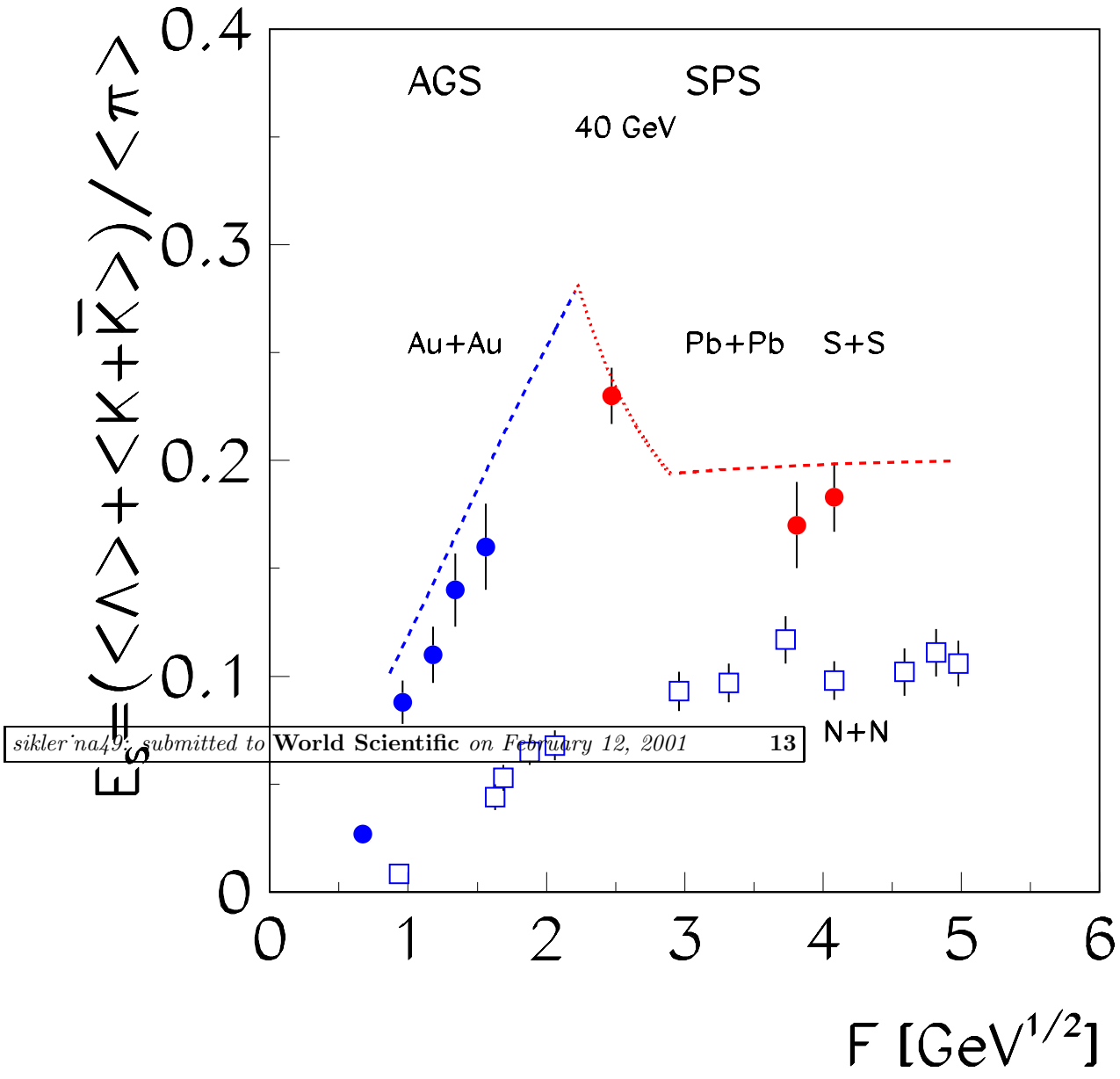




Figure 8. The dependence of *a)* the difference between pion to participant ratios – *b)* strangeness to pion ratio – for central A+A collisions and N+N interactions on the collision

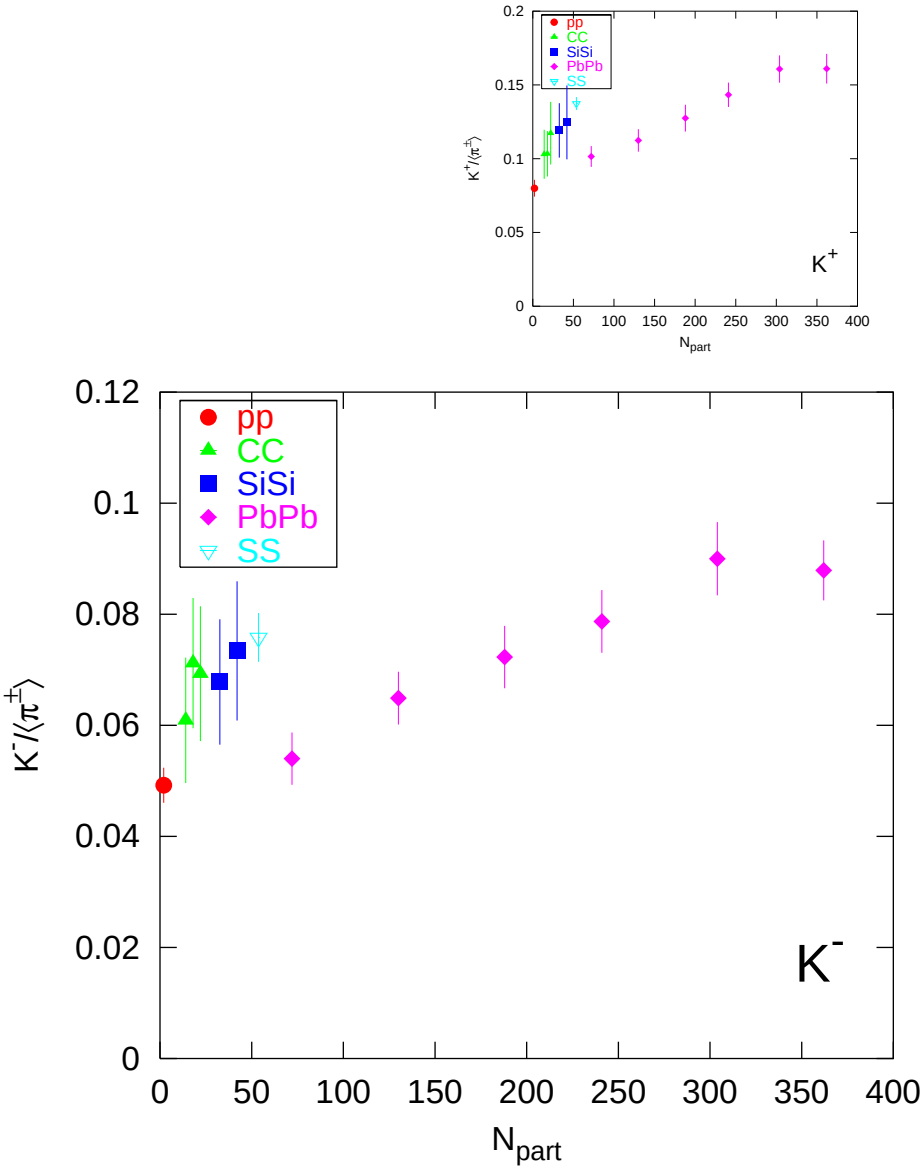


Figure 9. Ratios of $K^+/\langle\pi^\pm\rangle$ and $K^-/\langle\pi^\pm\rangle$ total yields as function of number of participants in nuclear collisions.

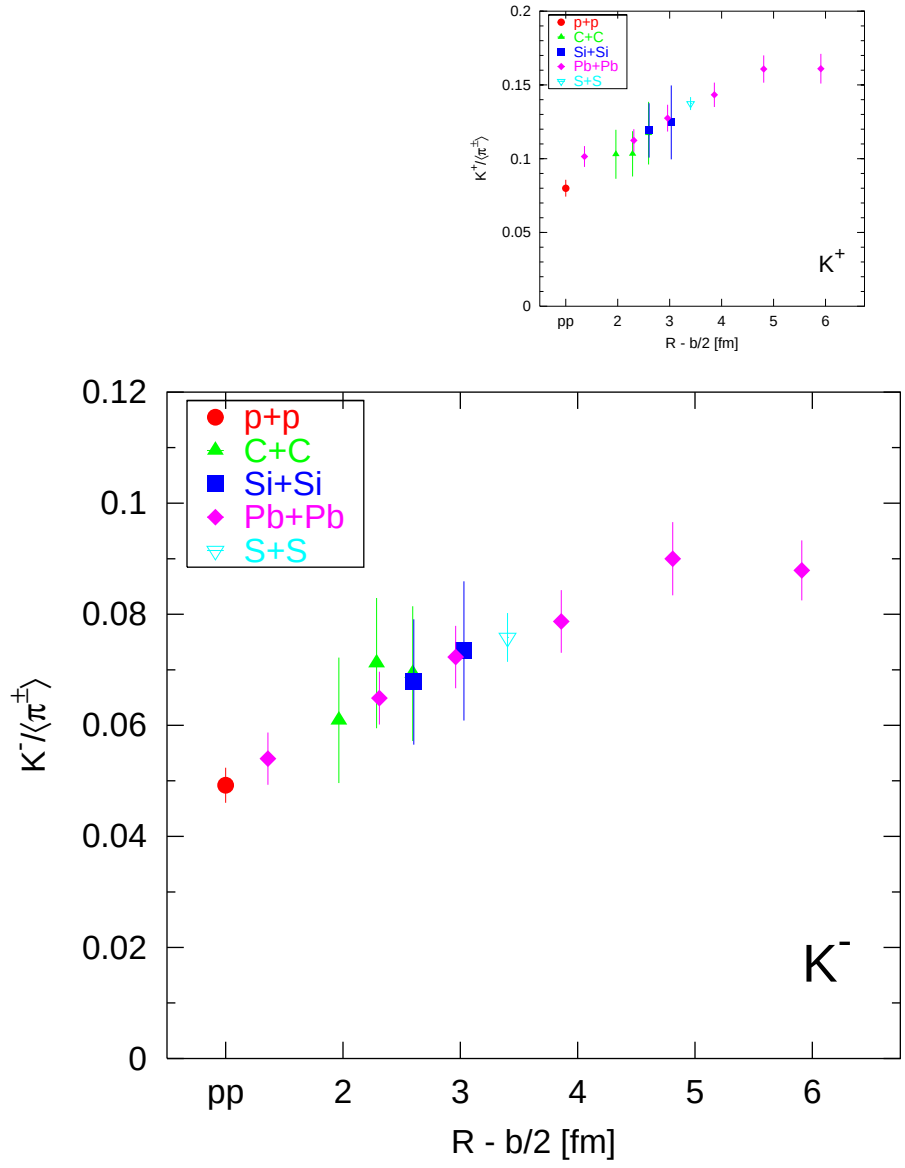


Figure 11. Ratios of $K^+/\langle\pi^\pm\rangle$ and $K^-/\langle\pi^\pm\rangle$ total yields as function of R-b/2 in nuclear collisions.